

# Sorting Fluorescent Nanocrystals Using DNA

*Daniele Gerion,<sup>\*†</sup> Wolfgang J. Parak,<sup>†</sup> Shara C. Williams, Daniela Zanchet, Christine  
M. Micheel, and A. Paul Alivisatos\**

Department of Chemistry, University of California, Berkeley, and Materials Sciences  
Division, Lawrence Berkeley National Laboratory, Berkeley, CA, 94720.

\* University of California, Department of Chemistry, Hildebrand B62, Berkeley, CA,  
94720.

Tel : (510) 642-7371; Fax : (510) 642-6911

E-mail: gerion@uclink4.berkeley.edu, alivis@uclink4.berkeley.edu

<sup>†</sup> Both authors contributed equally to this work.

## **Abstract**

Semiconductor nanocrystals with narrow and tunable fluorescence are covalently linked to oligonucleotides. These biocompounds retain the properties of both nanocrystals and DNA. Therefore, different sequences of DNA can be coded with nanocrystals and still preserve their ability to hybridize to their complements. We report the case where four different sequences of DNA are linked to four nanocrystal samples having different colors of emission in the range of 530-640 nm. When the DNA-nanocrystal conjugates are mixed together, it is possible to sort each type of nanoparticle using hybridization on a defined micrometer-size surface containing the complementary oligonucleotide. Detection of sorting requires only a single excitation source and an epifluorescence microscope. The possibility of directing fluorescent nanocrystals towards specific biological targets and detecting them, combined with their superior photo-stability compared to organic dyes, opens the way to improved biolabeling experiments, such as gene mapping on a nanometer scale or multicolor microarray analysis.

DNA microarray technology is an increasingly important tool since it considerably accelerates genetic analysis. It has been used for monitoring of gene expression, mutation detection, single nucleotide polymorphism analysis and many other applications.<sup>1</sup> It relies on hybridization between DNA sequences on the microarray and a fluorescent sample. Unfortunately, multicolor analysis using different dyes requires multiple excitation sources. Consequently, the microarray analysis system increases in complexity when several multiplexed channels are simultaneously recorded. This is illustrated by the recent development of a complex four-laser confocal system providing six different excitation wavelengths.<sup>2</sup> In order to simplify markedly the microarray systems and analysis, multiplex labeling scenarios call for an alternative technology to fluorescent dyes.

Core/shell CdSe/ZnS semiconductor nanocrystals are robust fluorescent probes with size tunable emission properties. Unlike dyes, they do not bleach significantly and their broad absorption spectrum allows the excitation of all the emission colors at once.<sup>3-6</sup> For these reasons, an intense research activity investigates their affinity in a variety of biological labeling scenarios.<sup>7-8</sup> Besides multicolor DNA array assays,<sup>1-2</sup> DNA conjugated semiconductor quantum dots may prove to be of use in multicolor gene mapping<sup>7,9</sup> and in spatial organization of nanocrystals.<sup>10-12</sup> These compelling goals require the ability to manipulate the nanocrystals of many sizes, to target and sort them into different specific locations using the recognition capability of the DNA.

In recent years, oligonucleotides have been linked to CdSe/ZnS nanocrystals in two ways. Both of them started by the solubilization of the nanocrystals by priming their surface with thiolated or bi-thiolated water-soluble molecules. In the very first report, Mitchell and coworkers used thiolated oligonucleotides to partially displace

mercaptopropionic acid molecules from the surface of the dots.<sup>12</sup> However, the presence of carboxyl groups on the surface of the nanocrystals was later reported to lead to strong nonspecific binding to the oligonucleotide probe backbone. To overcome this difficulty, Pathak and coworkers developed a strategy in which hydroxylated CdSe/ZnS nanocrystals were covalently attached to oligonucleotide sequences via a carbamale linkage.<sup>13</sup> Such DNA-nanocrystal conjugates were successfully used in a one-color fluorescence in-situ hybridization (FISH) assay with a minimum of nonspecific binding. However, high salt conditions inside the cells caused a partial agglomeration of the nanocrystals, most likely because of the dynamic binding between the nanocrystals and the bi-thiolated capping molecules. The agglomeration manifested itself in the variation of the fluorescence signal intensity. The use of semiconductor nanocrystals as multicolor biolabels requires both minimal nonspecific binding and stability of the nanoparticles in biological environments. Those stringent conditions have prevented in the past the use of CdSe/ZnS nanocrystals as multiplexed probes. Thus, such nanocrystals have been used only in a few simple experiments involving either nonspecific interaction<sup>8</sup> or one-color labeling.<sup>7,8,13-16</sup>

CdSe/ZnS nanocrystals with improved stability in physiological conditions have been produced by alternative water-solubilization methods. For instance, Mattoussi and coworkers engineered a positively charged protein which binds electrostatically to negatively charged carboxylated nanocrystals and confer stability to them in aqueous buffers.<sup>16</sup> Recently, our group described a different water-solubilization procedure which yielded stable solutions of CdSe/ZnS nanocrystals in up to 200 mM of NaCl as evidenced by gel electrophoresis studies.<sup>4</sup> Specifically, semiconductor nanocrystals are surrounded

by a thin silica shell which contains stabilizing polyethylene glycol (PEG) groups and derivatizable thiol groups on its surface. Such silanized nanocrystals exhibit no detectable nonspecific binding to oligonucleotides. Consequently, conventional heterobifunctional cross-linkers were used to covalently link the oligonucleotides to the nanocrystals.<sup>17</sup> The reaction yielded about 2-4 single-stranded DNA (ss-DNA) per nanoparticle and did not affect the bulk optical properties of the nanocrystals.

In this paper, we focus on the activity of such DNA-nanocrystal conjugates and the ability to sort them using the attached DNA. We show that because of the high stability of the nanocrystals in buffers and because of their weak nonspecific binding, multicolor targeting has been achieved for the first time. We base our conclusions on selective hybridization of DNA-nanocrystal conjugates on micrometer-size gold patterns which are then probed by fluorescence confocal microscopy. In particular, we report experiments in which four different sizes of DNA-labeled nanocrystals with different fluorescence colors are mixed in solution. The solution is then exposed to substrates on which different ss-DNA have been anchored on square pattern locations. The Watson-Crick interactions between the immobilized ss-DNA and the DNA-nanocrystal conjugates allow sorting of the nanocrystals. The ability to sort and specifically target multiple nanocrystal probes using short oligonucleotides may pave the way to gene mapping of combed DNA, with resolutions well below a few kilobases achieved with two-color dyes,<sup>7-9</sup> and multicolor DNA array studies with a single excitation source.<sup>1-2</sup>

To perform selective hybridization studies, or sorting experiments, we used a micrometer-size gold pattern grown on top of a silicon wafer using standard lithography techniques (Fig.1A). Each gold pattern has a square shape with a square inner hole,

which makes it easily identifiable. Gold provides an obvious choice for DNA immobilization since this process has been well documented.<sup>18-20</sup> The sorting experiment relies on the interaction between the nanoparticles and the gold surfaces mediated by the DNA. To investigate such an interaction, an Ar<sup>+</sup> laser ( $\lambda_{\text{exc}}=488$  nm) excites the nanocrystals on the gold pads and the resulting fluorescence is collected in a confocal microscope setup (Fig.1B). Images and spectra are recorded and analyzed using a liquid nitrogen cooled CCD camera. The next section provides a detailed description of the experimental procedures.

## **Experimental Procedure**

**The gold/silica substrates.** Gold squares are grown on top of a silicon wafer using standard lithographic techniques. Specifically, a 20 nm thick gold layer is deposited on top of a 10 nm thick chromium adhesion layer. The gold patterns are hollow squares of 8  $\mu\text{m}$  with a 4  $\mu\text{m}$  inner hole, 60  $\mu\text{m}$  apart from each other. A single substrate is about 40 x 40 squares and is about 2 x 2 mm.

**Activation of the gold substrates.** Gold/silicon substrates are washed 10 minutes in acetone, and then dipped in a piranha solution (~70% sulfuric acid, ~30 % hydrogen peroxide) for 5-8 minutes. After extensive washing with Millipore water, the substrates are immersed in 100  $\mu\text{l}$  of absorption buffer (500 mM K<sub>2</sub>HPO<sub>4</sub>, 500 mM KH<sub>2</sub>PO<sub>4</sub>, 500 mM NaCl, 0.1% v/v of Tween 20) in which 1-3  $\mu\text{M}$  of thiolated oligonucleotide has been dissolved. The substrates are left for about 2 hr, and then washed once in 2 ml of absorption buffer for 1 minute, and then 4 more times in 2 ml of water for 1 minute each. Each gold/silicon substrate is then dipped in a solution of passivation buffer (50 mM

phosphate buffer (PB), 150 mM NaCl, 0.1% v/v of Tween 20) with ~5 mM of mercaptohexanol, left for 1 hr, and then washed 5 times with 2 ml of Millipore water for 1-2 minutes each time. At this point, the substrates are used directly for hybridization of the nanocrystals.

**DNA-Nanocrystal conjugation.** Each emission color of nanocrystals is prepared with a different sequence following the procedures detailed in Refs.(4) and (17). Briefly, amino-terminated oligonucleotides (IDT Technologies Inc, Coralville, IA) are activated towards maleimide species by using sulfo-SMCC cross-linkers in large excess (>500 x). Maleimide-activated oligonucleotides are purified and isolated by anion exchange chromatography. The fractions of pure and maleimide-activated oligonucleotides can be fully separated; the latter have a larger elution time. Both fractions are unambiguously identified by MALDI-TOF spectroscopy. The maleimide-activated oligonucleotide solutions are extremely pure, with no excess of free cross-linker. The maleimide-activated oligonucleotide is reacted with a 10-20 fold excess over thiolated silanized nanocrystals. The formation of a covalent bond between the oligonucleotides and nanoparticles is ascertained by gel electrophoresis mobility measurements. Pure nanocrystals and nanocrystals incubated with oligonucleotides lacking the cross-linker activation exhibit exactly the same mobility pattern over a period ranging from 2 to 120 hrs. Conversely, nanocrystals incubated with 20-fold excess of maleimide-activated oligonucleotides exhibit a 20-50% increase in mobility, which is stable over at least 5 days. The data unambiguously indicate that oligonucleotides are covalently bonded to silanized nanocrystals.

**DNA-Nanocrystal solution preparation.** The oligonucleotide sequences attached to the nanocrystals are (5' to 3', X represents an amine used for covalently linking the nanoparticles): oligo-green = X AAA AAA CTT CGC ATT CAG GAT, oligo-yellow= GCC TAC GAG TTG AGA AAA AAA X, oligo-orange= X AAA AAA ATC CTG AAT GCG TGA, oligo-red=GCT TGA CTC GTA GTG AAA AAA X. Oligo-nanocrystal solutions are purified through a Sephadex G200 gel equilibrated in 10 mM PB, pH~7.2, and then condensed to a volume of ~ 100  $\mu$ l in Microcon 100 centrifuge filters resulting in a ~1-5  $\mu$ M solution of nanocrystals. The solution eluted through the Microcon 100 device has no absorbance at 260 nm. We therefore estimate that the concentration of unbound maleimide-activated oligonucleotide is well below 1 nM.

**Hybridization of Nanoparticles.** DNA-nanocrystal solutions of four different colors, each prepared as described above, are mixed together. This mixed solution is brought to 10 mM PB, 50 mM NaCl, 0.1% v/v Tween 20. The final concentration of nanoparticles in the hybridization step is about 20 nM for each color. The exact concentration is chosen such that each color contributes equally to the fluorescence. In the particular case of Fig.3a, the concentration of each color of emission is: green 45 nM; yellow: 37.5 nM; orange: 6.8 nM; red: 10 nM. The substrates are then dipped in the hybridization solution. Since the measured melting temperature of the diverse oligonucleotide sequences is around  $T_m \sim 42^\circ\text{C}$  with a width of  $\Delta T \sim 15^\circ\text{C}$ , the substrates are first sit for 1 hr at room temperature and then overnight at  $4^\circ\text{C}$ . The substrates are then washed four times in 1.5 ml of 100 mM PB, 300 mM NaCl, 0.1% v/v Tween 20. They are then transferred into a quartz cell filled with 100 mM PB, 300 mM NaCl, where they are imaged. Imaging in dry conditions is also possible with, however, a slightly lower overall signal. In that case,

the substrates are washed one more time in 100 mM PB, 100 mM NaCl for ~1 minutes and then gently dried with a Kimwipe.

**Imaging Processing.** The wet cell is mounted in front of a 60x, 0.7 NA air objective. We use an Ar<sup>+</sup> laser for excitation (~ 0.5 mW,  $\lambda_{exc}=488$  nm) in a confocal configuration as shown in Fig. 1B. The outgoing fluorescence light is focused on a liquid nitrogen cooled CCD camera (Acton research SpectraPro –300i from Roper Scientific, Tucson AZ). For each image, the capture time is 1 to 5 seconds and is indicated in the captions. To measure the fluorescence spectrum, the slits in front of the detector are closed so as to isolate only the square pattern. The CCD camera is switched into “spectroscopy” mode by inserting a 300 groove grating. Resolution on the fluorescence spectrum is about 2 nm.

## Results and discussion

We will show later that multicolor specific hybridization of DNA-nanocrystals has been achieved as a result of a careful study of the hybridization conditions for each color of DNA-nanocrystals separately. Thus, we will first illustrate the specific hybridization activity of DNA-nanocrystal conjugates by considering the example of green emitting dots (Fig.2). We investigated four possible scenarios. In the first, the gold patterns contained the oligonucleotide sequence complementary to that on the nanocrystals. Then, we considered two control cases where either the nanoparticles or the gold substrates did not bear DNA. Finally, we looked at the control case where the oligonucleotide sequences on the nanocrystals and on the gold patterns did not match at all. As shown in Fig. 2A, fluorescence from the gold patterns shows up distinctly when the oligonucleotides on the nanoparticles are complementary to the ones on the metal

surface. In this positive case, the signal to noise ratio was deduced from cross-section intensities across the squares (Fig. 2E) and ranged from 2 to 10. Unfortunately, we were not able to determine the number of emitters from the surface. A simple estimate indicated that about  $10^5$  close-packed nanoparticles could assemble on each gold pattern, but the number of nanoparticles that hybridize and contribute to the emission signal is certainly smaller, possibly around 15% of a densely-packed layer of particles.<sup>21</sup> Control experiments demonstrate that nonspecific interaction is minimal. In particular, if no DNA is present on the particles (Fig. 2B) or on the gold substrate (Fig. 2C), the fluorescence emission is vanishingly small with only a very few gold patterns having a faint, barely detectable fluorescence. Similarly, a random strand on the gold surface does not recognize the nanoparticles (Fig. 2D). The positive hybridization assays, performed with each emission color, clearly demonstrate that the bioactivity of the ss-DNA is maintained despite the semiconductor nanocrystals.

The concentration of the nanoparticles in solution plays a critical role for efficient hybridization. High concentrations of nanoparticles ( $\gg 200$  nM) usually produce a fluorescence shadow all over the substrates, while at low concentrations ( $\ll 100$  pM) we observe almost no fluorescence from the gold squares. This is likely related to the poor efficiency of the hybridization of DNA-nanocrystal conjugates on the gold surface since each nanocrystal bears only a few oligonucleotides. Indeed, low hybridization efficiencies have been observed for 10 nm gold nanocrystals bearing exactly 1, 2 or 3 DNA strands.<sup>22</sup> In contrast, 13 nm Au nanocrystals with about 220 DNA reportedly hybridize at femtomolar concentration.<sup>23</sup> In our experiments, concentrations of about 10-100 nM produce the best results. These concentrations correspond to the concentrations

of DNA used in some micro-array experiments.<sup>1,2,24-25</sup> Notice moreover that DNA-nanocrystal samples showed negligible nonspecific binding in the control experiments. This comes from the hydrophobic passivation of the gold patterns by mercaptohexanol molecules after ss-DNA absorption. Therefore, mild washing conditions are sufficient to remove most nonspecifically bound DNA-nanocrystal conjugates from the substrates.

The successful result of the one-color hybridization experiment suggests that DNA-nanocrystal conjugates could be of use in multicolor microarray studies. To address this issue, we investigated the possibility of sorting DNA-nanocrystal conjugates of different emission colors on specific locations using the selective hybridization of their DNA. Therefore, we prepared separately four different batches of nanocrystals, each covalently linked to a different oligonucleotide sequence of 21 bases. The emission colors of the samples are centered in the green, yellow, orange and red spectral range, respectively, and are easily resolved by the eye. However, due to the width of the fluorescence emission, adjacent channels partially overlap, as illustrated in Fig.3A. This figure also shows the fluorescence of the four DNA-nanocrystal conjugate solutions mixed together. This mixture was exposed to four different gold substrates, each separately activated with a different DNA. After hybridization occurs, each substrate is examined in an epifluorescence microscope through a 10x objective. The gold squares exhibit a fluorescence emission which is unambiguously related to the DNA sequence they are coated with (Fig.3B). For instance, gold patterns bearing the oligonucleotide sequence complementary to the one attached to green nanoparticles fluoresce green.

Further quantitative insight into the sorting efficiency is obtained by recording the spectrum of light coming from each square. These spectra are shown in Fig. 3C. For each

set of substrates, the square's emission dramatically narrows compared to the mixture solution, and it is clearly distinguishable from the fluorescence of the other substrates. Indeed, a deconvolution of the emission peak into fluorescence profiles from pure nanocrystal components (Fig.3A) indicates that greater than 70 to 95 % of the emission light comes from only one type of DNA-nanocrystal conjugate. The remaining 5% to 30% originates mainly from adjacent color channels. We believe therefore that the deduced efficiency is limited by cross-talk between adjacent channels, since it is difficult to deconvolute the fluorescence spectrum into two adjacent spectra by our numerical method of analysis. To get a percentage above 95%, it would be necessary to work with nanocrystals samples having less spectral overlap. With the present size distribution, this would limit to 3 the number of useful channels possible in the wavelength range from 530 to 640 nm. This number can be extended, in principle, since wet chemistry techniques allow the synthesis of nanoparticles emitting in the blue-UV (i.e. CdS, ZnSe) and in the red and near IR (i.e. InP), thereby not overlapping with nanoparticles emitting in the visible. Alternatively, it may be possible to further narrow the emission of each sample, but it is important to recall that this is more difficult in the multiple shell samples employed for biological labeling.

It is interesting to notice that, unlike some dyes, the metal surface does not quench the fluorescence of the silanized nanocrystals. Indeed, fluorescence spectra of DNA-nanocrystal conjugates in solution and on metal surfaces have virtually the same pattern (average emission wavelength, full width at half maximum), but not necessarily the same intensity. We cannot exclude the possibility of increased fluorescence intensity, or a decrease in intensity due to partial FRET, or other mechanisms of energy transfer

between the nanoparticles and the metal surface.<sup>26</sup> However, the energy transfer efficiency drops off as  $1/d^6$  where  $d$  is the distance to the surface. Considering the oligonucleotide plus cross-linker lengths ( $\sim 9$  nm) and the size of the nanoparticles ( $>7$  nm in diameter), the energy transfer should not be significant. These phenomena may be further studied by time-dependent measurements such as lifetime measurements.

The use of multicolor DNA-nanocrystal conjugates in DNA microarray technology still has some obstacles to overcome. For instance, selective hybridization of DNA-nanocrystal conjugates on gold patterns do not yet reach single base pair mismatch detection. We believe that such a result is possible by careful exploration of experimental conditions. Our current approach, with only one kind of ss-DNA per substrate does not allow fast and efficient screening of different conditions. Therefore, we turned to the conventional DNA microarrays printed on glass slides. On a single slide, we can probe a large number of DNA sequences and many different hybridization conditions at once. Our very preliminary results with a single color of nanoparticle confirm the results presented in Fig. 2 for gold patterns, but we still have not found the conditions for single nucleotide mismatch detection.<sup>27</sup> We stress, however, that with our current protocols, DNA-nanocrystal conjugates may be used in multicolor prescreening tests to differentiate random sequences of DNA.

Our experiments clearly prove that multicolor sorting is feasible. Four nanocrystals with spectrally resolved emission colors and bearing different oligonucleotides can be specifically directed towards different positions. Since those nanocrystals are about 7 to 14 nm in diameter,<sup>4</sup> it may be possible to control their positioning to within a few tens of nanometers. This suggests exciting applications in genetics. Large amounts of DNA can

be combed on surfaces, and subsequently probed at several kilobase resolution using organic dyes.<sup>9</sup> Since it has recently been shown that multicolor detection using nanocrystals can achieve unprecedented resolution of a few tens of nanometers,<sup>28</sup> it may be possible to perform gene mapping using two- or multi-color nanocrystals below the kilobase limit.

## **Acknowledgments**

We are grateful to Guanhua Wu for providing us the silicon/gold substrates, to Jiangtao Hu for help with the confocal setup and to Yin Thai Chan, Matthew Francis and Sarah Goh for valuable suggestions. We are also grateful to Xavier Michalet for reading the manuscript, for making so many valuable comments and suggestions and for his continuous interest in our work. S.C.W. acknowledges the Lawrence Livermore National Laboratory and the National Physical Science Consortium for financial support. D.Z. is grateful to FAPESP, proc. 99/08603-7. C.M.M is a Howard Hughes Medical Institute Predoctoral Fellow. This work was supported by NIH National Center for Research Resources, Grant Number 1 R01 RR-14891-01 through the U.S. Department of Energy under Contract No. DE-AC03-76SF00098.

## Figure Captions

**Figure 1.** (A) A schematic view of the gold patterns on a silicon wafer. The wafer is 2 mm x 2 mm and has about 40 x 40 gold patterns per wafer. (B) The setup for image capture and spectral measurements. A laser beam ( $\text{Ar}^+$ ,  $\lambda=488$  nm, 0.5 mW) is directed onto the sample using a dichroic mirror (DM) and then is focused on the sample through an objective (60 x magnification, NA=0.7). The fluorescent light is collected by the objective, is passed through a notch filter (NF) to suppress any remaining excitation light and is focused on the CCD detector by a focusing lens (FL). Two adjustable slits in front of the CCD camera (or pinhole P) allow rejection of most of the out-of-focus background. The CCD camera can be switched to spectroscopic mode by inserting a 300 groove grating. For a typical measurement, the objective is scanned over the surface until it finds a fluorescent pattern. It is then moved back and forth with a computer-controlled micrometer-resolution motor to focus the image. X-Y stages with micrometer-resolution allow scanning the surface to find other fluorescent squares.

**Figure 2.** Hybridization and control experiments with a green nanocrystal solution (emission  $\sim 544$  nm) exposed to 4 different substrates. Capture time is 0.5 sec. (A) Four examples of the substrate containing an oligonucleotide which is complementary to the one on the nanocrystals. The arrows indicate horizontal linescans to determine the signal to noise ratio in Fig. 2E. Examples where (B) the substrate has no oligonucleotides on it; (C) the nanoparticles have no DNA, but the substrate has DNA; (D) the substrate and the

nanoparticles have both non-complementary oligonucleotides. (E) Two linescans through figure 2A which indicate a signal to noise ratio of about 4.

**Figure 3.** (A) The fluorescence of the solution (in black) is the superposition of the fluorescence of four different DNA-nanocrystals samples. All spectra are normalized. (B) The same solution is exposed to four substrates, each being activated with a different oligonucleotide. The gold patterns exhibit a strong fluorescence with a minimal background signal. The capture time is 5 seconds. (C) The fluorescence spectrum of the squares (color) shows significant narrowing compared to that of the solution (black), and each set of squares has a characteristically different spectrum. Note the slight asymmetry of the fluorescence emission of the substrate sorting the orange nanocrystals. In this case, ~70% of the emission is from orange nanocrystals while ~30% are either from red or yellow contributions. For the other substrates, more than 90-95 % of the fluorescence is due to a single color of nanocrystals.

## References

- (1) (a) Review articles on DNA arrays have been published in a supplement issue of *Nature Genetics* **1999**, *21*. (b) Niemeyer, C.M.; Blohm, D. *Angew. Chem. Int. Ed.* **1999**, *38*, 2865-2869.
- (2) Graves, D.J.; Su, H.-J.; Addya, S.; Surrey, S.; Fortina, P. *BioTechniques* **2002**, *32*, 346-354.
- (3) Dabbousi, B.O.; Rodriguez-Viejo, J.; Mikulec, F.V.; Heine, J.R.; Mattoussi, H.; Ober, R.; Jensen, K.F.; Bawendi, M.G. *J. Phys. Chem. B* **1997**, *101*, 9463-9475.
- (4) Gerion, D.; Pinaud, F.; Williams, S.C.; Parak, W.J.; Zanchet, D.; Weiss, S.; Alivisatos, A.P. *J. Phys. Chem. B* **2001**, *105*, 8861-8871.
- (5) Han, M.; Gao, X.; Su, J.Z.; Nie, S. *Nature Biotech.* **2001**, *19*, 631-635.
- (6) Rosenthal, S.J. *Nature Biotech.* **2001**, *19*, 621-622.
- (7) Michalet, X.; Pinaud, F.; Lacoste, T.D.; Dahan, M.; Bruchez, M.P.; Alivisatos, A.P.; Weiss, S. *Single Mol.* **2001**, *2*, 261-276.
- (8) Bruchez, M.P.; Moronne, M.; Gin, P.; Weiss, S.; Alivisatos A.P. *Science* **1998**, *281*, 2013-2016.
- (9) Michalet, X.; Ekong, R.; Fougerousse, F.; Rousseaux, S.; Schurra, C.; Hornigold, N.; Slegtenhorst, M.v.; Wolfe, J.; Povey, S.; Bensimon, A. *Science* **1997**, *277*, 1518-1523.
- (10) Alivisatos, A.P.; Johnsson, K.P.; Peng, X.; Wilson, T.E.; Loweth, C.J.; Bruchez, M.P.; Schultz, P.G. *Nature* **1996**, *382*, 609-611.
- (11) Loweth, C.J.; Caldwell, W.B.; Peng, X.; Alivisatos, A.P.; Schultz, P.G. *Angew. Chem., Int. Ed.* **1999**, *12*, 1808-1812.

- (12) Mitchell, G.P.; Mirkin, C.A.; Letsinger, R.L. *J. Am. Chem. Soc.* **1999**, *121*, 8122-8123.
- (13) Pathak, S.; Choi, S.-K.; Arnheim, N.; Thompson, M.E. *J. Am. Chem. Soc.* **2001**, *123*, 4103-4104.
- (14) Chan, W.C.-W.; Nie S. *Science* **1998**, *281*, 2016-2018.
- (15) Winter, J.O.; Liu, T.Y.; Korgel, B.A.; Schmidt, C.E. *Adv. Mater.* **2001**, *13*, 1673-1677.
- (16) Mattoussi, H.; Mauro, J.M. ; Goldman, E.R.; Anderson, G.P.; Sundar, V.C.; Mikulec, F.V.; Bawendi, M.G. *J. Am. Chem. Soc.* **2000**, *122*, 12142-12150.
- (17) Parak, W.J.; Gerion, D.; Zanchet, D.; Woerz, A.S.; Micheel, C.M.; Williams, S.C.; Seitz, M.; Bruehl, R.E.; Bryant, Z.; Bustamante, C.; Bertozzi, C.R.; Alivisatos, A. P. *Chem. Mater.* Accepted for publication.
- (18) Peterlinz, K.A.; Georgiadis, R.M.; Herne, T.M. ; Tarlov, M.J. *J. Am. Chem. Soc.* **1997**, *119*, 3401-3402.
- (19) Herne, T.M.; Tarlov, M.J. *J. Am. Chem. Soc.* **1997**, *119*, 8916-8920.
- (20) Levicky, R.; Herne, T.M.; Tarlov, M.J.; Satija S.K. *J. Am. Chem. Soc.* **1998**, *120*, 9787-9792.
- (21) Willner, I.; Patolsky, F.; Wasserman, J. *Angew. Chem., Int. Ed.* **2001**, *40*, 1861-1864.

(22) (a) Zanchet, D.; Micheel, C.M.; Parak, W.J.; Gerion, D.; Alivisatos, A.P. *Nano. Lett.* **2001**, *1*, 32-35; (b) Zanchet, D.; Micheel, C.M.; Parak, W.J.; Gerion, D.; Alivisatos, A.P. unpublished.

(23) Taton, T.A.; Mirkin, C.A.; Letsinger, R.L. *Science* **2000**, *289*, 1757-1760.

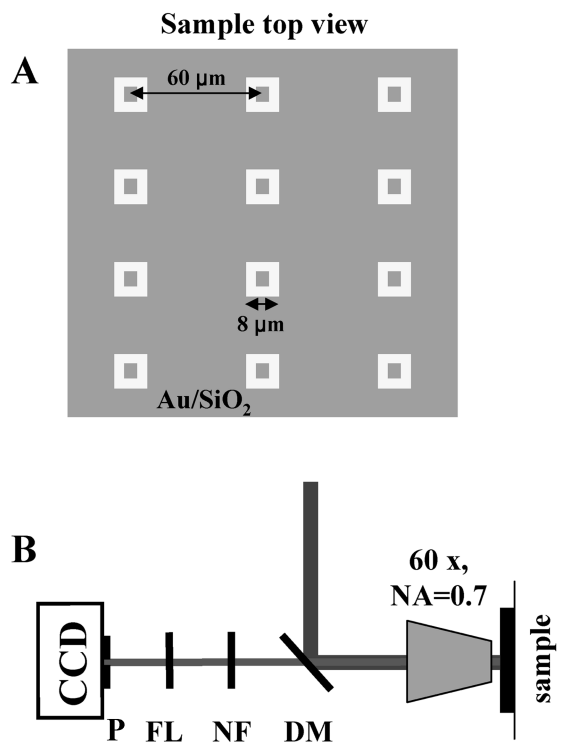
(24) Taton, T.A.; Lu, G.; Mirkin, C.A. *J. Am. Chem. Soc.*, **2001**, *123*, 5164-5165.

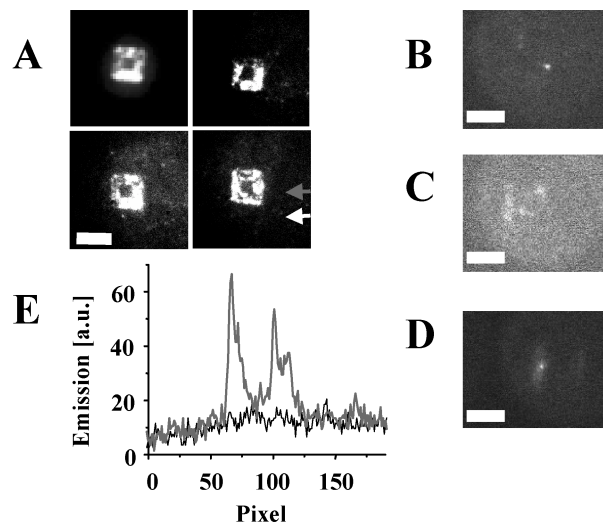
(25) Heller, M.J.; Tu, E.; Holmsen, A.; Sosnowski, R.G.; O'Connell J. in *DNA microarrays, a practical approach*, ed. M. Schena, (Oxford University Press Inc., New York), **1999**, pp.167-185.

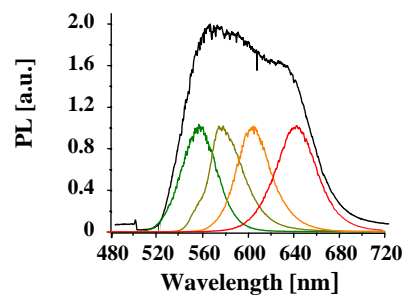
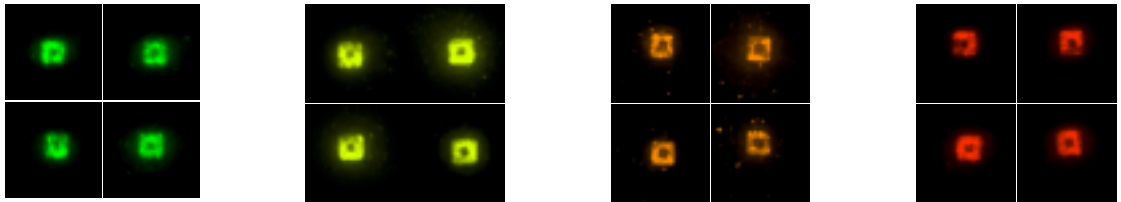
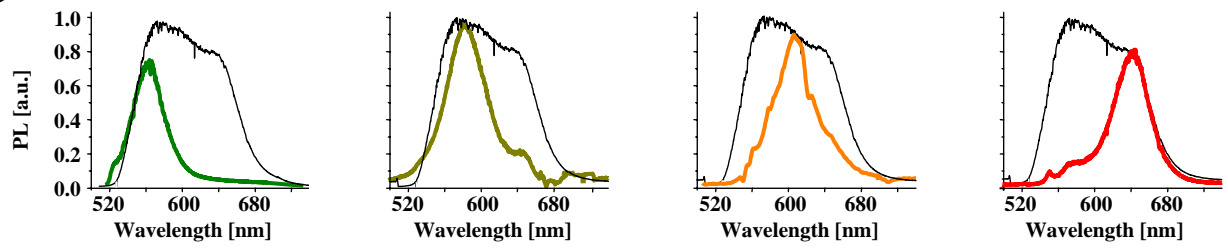
(26) Lakowicz, J.R. *Anal. Biochem.* **2001**, *298*, 1-24 and references therein.

(27) Gerion, D; Chen, F. *et al.* unpublished.

(28) Lacoste, T.D.; Michalet, X.; Pinaud, F.; Chemla, D.S.; Alivisatos, A.P.; Weiss, S. *Proc. Natl. Acad. Sci. USA* **2000**, *97*, 9461-9466.





**A****B****C**

**Table of Contents graphic**

